

Calibration of a SiPM-on-Tile muon calorimeter for high-altitude ballooning applications

Saskia Põldmaa, Mihkel rannut, Ralf Robert Paabo,
Violeta Jürgens, Mattias Jõgi

April 10, 2024

1 Introduction

Most particles can be absorbed in calorimeters, which enables us to measure their energy. Muons, however, can pass through big solid structures, including calorimeters. This is why muon calorimetry usually requires the use of big systems of magnets. This approach is not suited for high-altitude ballooning, where the mass of the apparatus is critical. Scintillator tiles however are lightweight yet just thick enough so that the energy deposited in them is considerable enough to measure.

We stumbled upon this problem after conducting a stratospheric flight with our homemade muon detectors. Although our initial goal was to measure only the change in count rate as the detector ascended, we also observed a promising behaviour of the voltage spectrum. This is why we are hopeful that in our upcoming stratospheric flights we could interpret the voltage spectrums as the changing spectrums of cosmic ray muons. This would be an accessible way to shed light onto how fast the energy loss truly is and what is the most populous muon energy at each altitude.

2 Previous results

We were able to build our own detector thanks to the documentation of the CosmicWatch [4] project. Our detectors deviate from the CosmicWatch

ones electronics-wise (see for circuit diagram) but they are still built upon a scintillator coupled with a SiPM and an Arduino Nano for processing the pulses. The final two detectors which were used in coincidence mode onboard the stratospheric flight are shown in Figure 1.

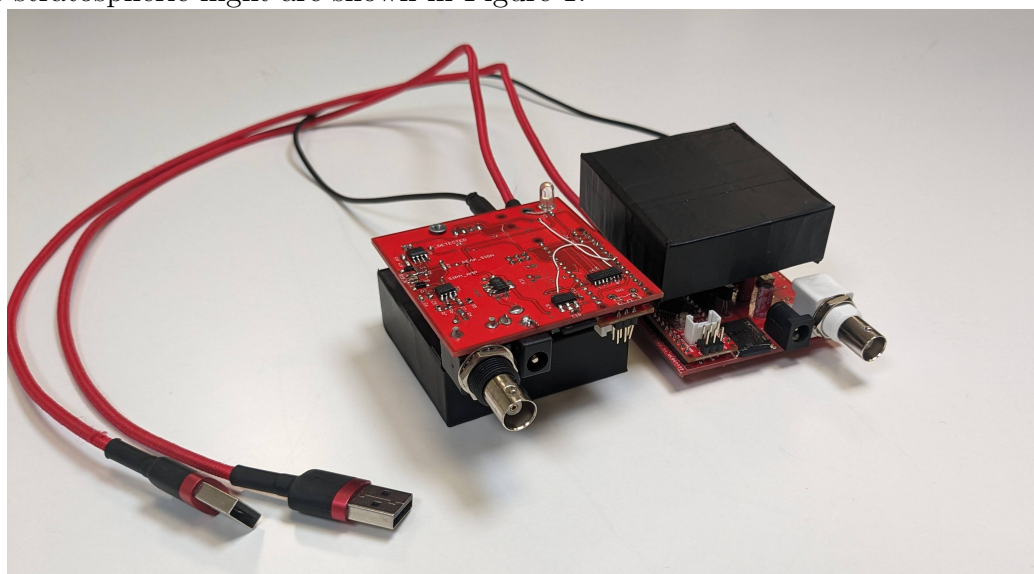


Figure 1. Our two muon detectors.

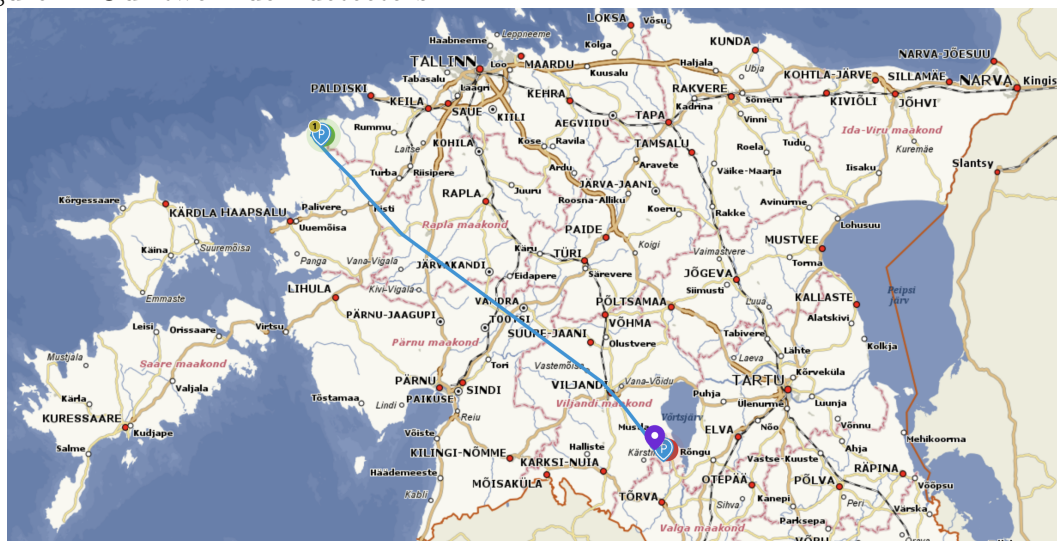


Figure 2. Flight path.

The stratospheric flight was successful as we were able to gather data at heights up to 24km above the sea level while the detector flew over Estonia

as seen in Figure 2. The Regener-Pfotzer maximum was observed to start at 13.3km. The observed and theoretical count rates are given in Figure 3. The theoretical count rate was based on the Tang model [8] for muon intensity, from which we calculated the expected count rates taking into account the decay and energy loss of muons (see for calculations). The best fit line in the Figure 3 was found for the function

$$f(h) = f(0) \exp\left(\frac{h}{c\gamma\tau}\right) = f(0) \exp\left(\frac{m_\mu ch}{E\tau}\right) \quad (1)$$

where $f(h)$ is the count rate at altitude h , c the speed of light, γ the Lorentz factor, τ the lifetime at rest of muons, m_μ the rest mass of muons and E the energy of muons. The count rate follows this function if all the muons were i) vertical and ii) at the same never-changing energy E which from the best fit line was found to be 989.5 MeV.

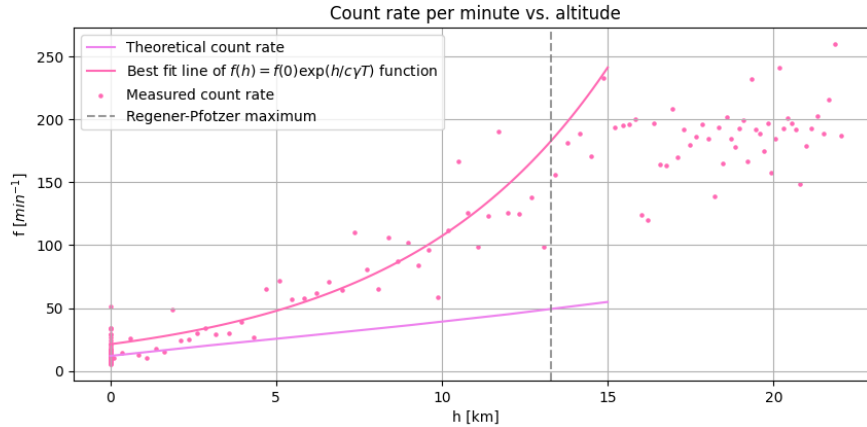


Figure 3. Count rates for altitudes up to 24km.

The theoretical approach which was based on the Tang’s model for muon intensity, is also sufficient to calculate the ”spectrum of energy deposited in scintillator” as shown in Figure 4. For this, the deposited energy is calculated from the muon energy via the Bethe-Bloch formula. We have assumed that the energy loss is purely due to ionization.

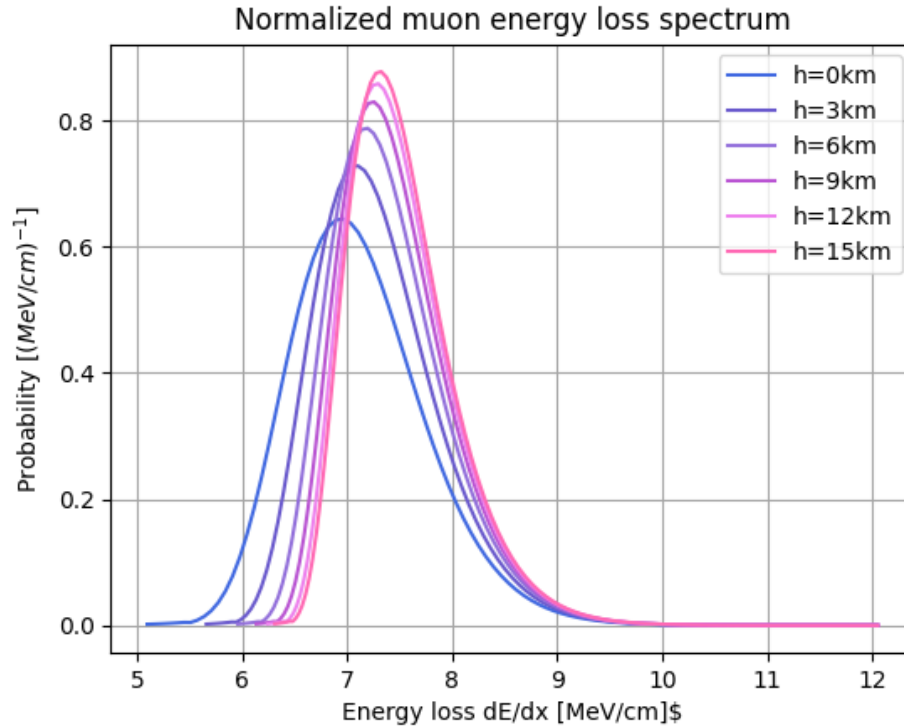


Figure 4. Deposited energy spectrum at various altitudes, normalized to unit area.

Although our model wasn't sufficient for the count rate due to simplifying all of the muons as being zenith-directional, it gives a good estimate for the deposited energy as a function of height: as seen in Figure 5, an increase in altitude shifts the voltage spectrum towards higher voltages. This corresponds well with Figure 4, which tells us that the energy a muon deposits is also increasing. It can be seen that the muon peak is clearly separated from the low energy part which caused by the radioactivity background.

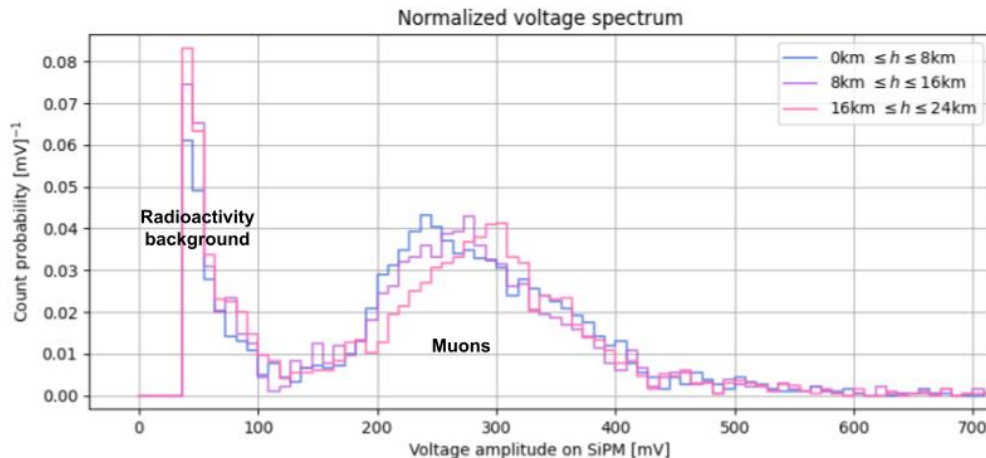


Figure 5. Voltage spectrums measured at altitudes 0÷24 km, normalized to unit area.

3 Carrying out the measurement

To interpret voltage as the muon’s energy, one must first calculate the energy deposited in the scintillator via the muon energy and secondly determine the pulse’s voltage amplitude due to the deposited energy. The former can be done analytically using the Bethe-Bloch formula, however the latter is most affected by the detector’s setup and must be determined empirically.

That is why we wish to measure the relationship between the energy deposited via ionization and the created voltage in the SiPM. A muon beam will be created by closing the collimator - this approach was chosen over the muon filter as the resulting flux of 100 to 1000 particles per spill [6] is sufficiently low for digital readout. The resulting flux (0.1÷10GeV) covers all of the muon energies that we are interested in: 4.8GeV - spectrum maximum at sea level [8], 7GeV - spectrum maximum at Regener-Pfotzer maximum [3] and 990MeV - spectrum maximum calculated from count rate.

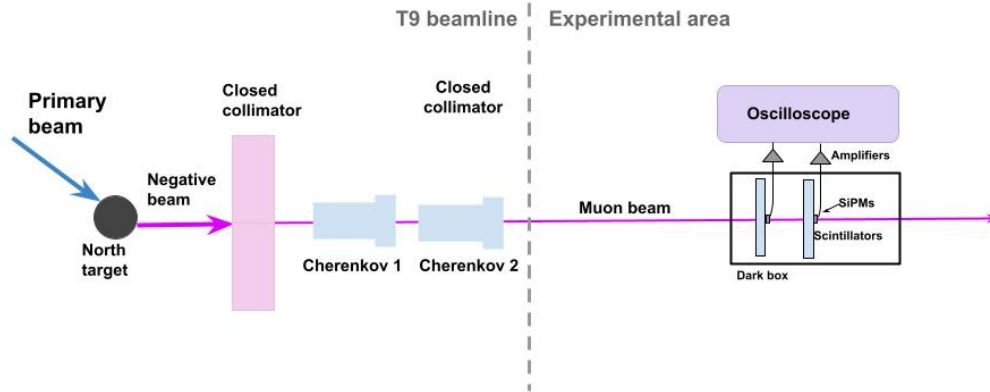


Figure 6. Setup of the beamline.

The DUT will consist of two coincidence detectors utilizing the same SiPM that we have used so far - the Hamamatsu S14161-4050HS-06, a plastic scintillator similar to our previously used Advantech's ATP-50515 (which is no longer sold) and an oscilloscope for the readout. The shielding from visible light is crucial, that is why a light-tight box around the apparatus is necessary.

Table 1. Scintillator parameters

Property	Value
Light Yield (Photons/MeV)	$\sim 64\%$ than $C_{14}H_{10}$
Wavelength Emission	423 nm
Rise Time	0.9 ns
Decay Time	2.3 ns
Light Attenuation	210 cm

The scintillator will be wrapped in DF2000MA film because this gave us a voltage spectrum maximum 32mV higher compared to aluminum foil, indicating better reflection. The scintillator's face side is 6×6 cm and the width 2 cm. For optimal light collection the SiPM will be placed in a dimple. The dimensions of the dimple shown in Figure 7 were chosen by rescaling the size of the Mainz dimple for a 1×1 mm² SiPM in [7] in accordance to our SiPM's effective area of 4×4 mm².

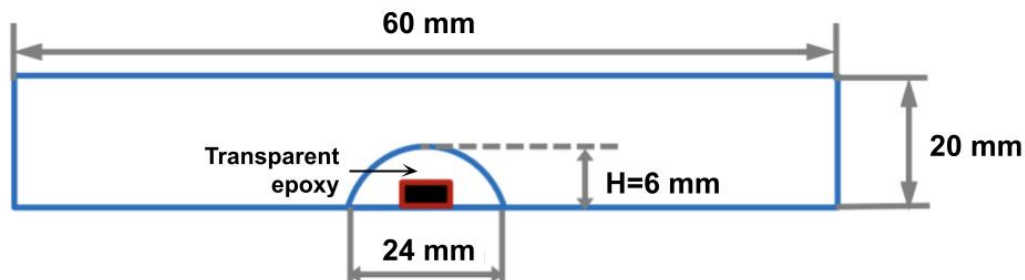


Figure 7. SiPM in dimple.

The two Cherenkov detectors will be set to slightly different pressures as to select a momentum range for measurements. For measurements centered around $4.8\text{GeV}/c$ and $7\text{GeV}/c$ CO_2 will be used but at $990\text{ MeV}/c$ C_3F_8 will be needed instead. The muon spectrum of the beam is not well known. While we would gather data about the spectrum during the course of our measurements, the Figure 9 is used for now as an estimate for the needed pressure difference to keep the number of particles in the selected momentum range at about 10 particles per spill (assuming there are 1000 per spill in total).

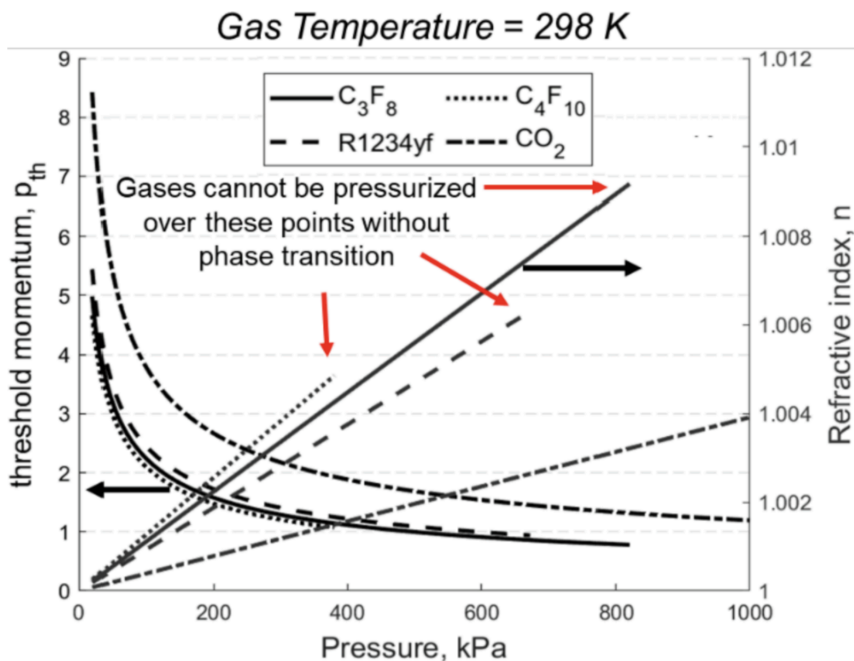


Figure 8. Cherenkov threshold muon momentum and refractive index for

C_3F_8 , $R1234yf$, C_4F_{10} , and CO_2 gas radiators as a function of gas pressure.
Chatzidakis 2022.[5]

Muon spectrum

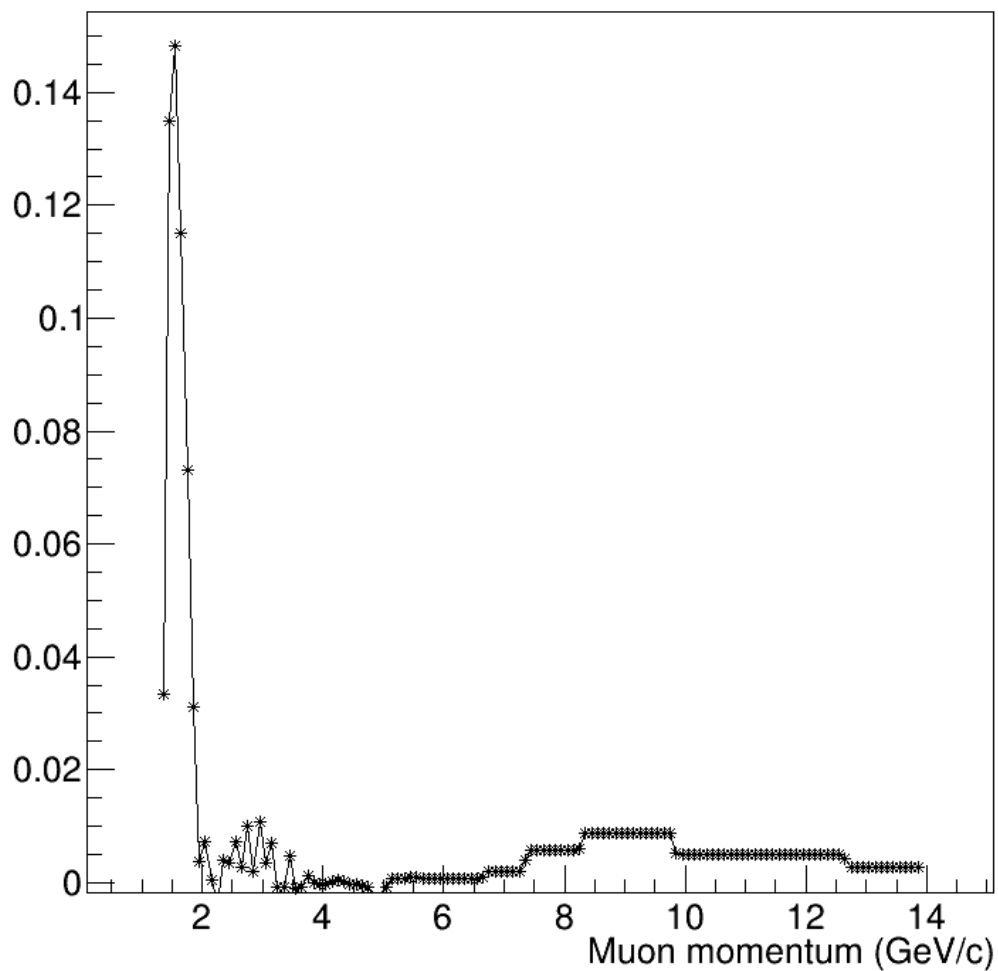


Figure 9. Muon spectrum at T10. Email with Martin S.

Table 2. Cherenkov detector pressures for muon momentum measurements.

Momentum	Gas	Momentum difference	Pressures in Cherenkov detectors
7 GeV/c	CO_2	2 GeV/c	0.18 & 0.39 bar
4.8 GeV/c	CO_2	1 GeV/c	0.42 & 0.99 bar
990 MeV/c	C_3F_8	300 MeV/c	3.60 & 6.81 bar

Note that at 4.8 GeV/c the momentum difference was found to be 15 GeV/c but was then changed to 1 GeV/c by comparison to the other two data points.

After the particles in the selected momentum ranges are identified by emittance of light in only one but not the other Cherenkov detector, they will once again be traced down in the DUT and the voltage that they create on the SiPM will be measured. The measured voltages can then not only be compared to the voltage peaks in cosmic ray measurements but also to the total voltage spectrum created by the T9 or T10 muon beams.

References

- [1] N. Akchurin, K. Carrell, J. Hauptman, H. Kim, H.P. Paar, A. Penzo, R. Thomas, and R. Wigmans. Muon detection with a dual-readout calorimeter. *Nuclear Instruments and Methods in Physics Research Section A: Accelerators, Spectrometers, Detectors and Associated Equipment*, 533(3):305–321, 2004.
- [2] Miguel Arratia, Bruce Bagby, Peter Carney, Jiajun Huang, Ryan Milton, Sebouh J. Paul, Sean Preins, Miguel Rodriguez, and Weibin Zhang. Beam test of the first prototype of sipm-on-tile calorimeter insert for the eic using 4 gev positrons at jefferson laboratory. *Instruments*, 7(4), 2023.
- [3] Dimitra Atri and Adrian L. Melott. Modeling high-energy cosmic ray induced terrestrial muon flux: A lookup table. *Radiation Physics and Chemistry*, 80(6):701–703, 2011.
- [4] Spencer N. Axani. The physics behind the cosmicwatch desktop muon detectors, 2019.
- [5] Junghyun Bae and Stylianos Chatzidakis. Development of compact muon spectrometer using multiple pressurized gas cherenkov radiators. *Results in Physics*, 39:105771, 2022.
- [6] CERN. Information about the t9 beam line and experimental facilities, 2019.

- [7] Yong Liu. Designs and measurements of dimpled scintillator tiles with smd sipms. *CALICE Collaboration Meeting*, September 2014.
- [8] Alfred Tang, Glenn Horton-Smith, Vitaly A. Kudryavtsev, and Alessandra Tonazzo. Muon simulations for super-kamiokande, kamland, and chooz. *Physical Review D*, 74(5), September 2006.